Robotica (2015) volume 33, pp. 19–39. © Cambridge University Press 2014
doi:10.1017/S0263574714000034

Development of a whole arm wearable robotic exoskeleton for rehabilitation and to assist upper limb movements

M. H. Rahman†,‡*, M. J. Rahman†, O. L. Cristobal†, M. Saad†, J. P. Kenné† and P. S. Archambault‡,§

†*Department of Electrical Engineering, École de Technologie Supérieure (ETS), Montréal, Canada*
‡*School of Physical & Occupational Therapy, McGill University, Montréal, Canada*
§*Interdisciplinary Research Center in Rehabilitation (CRIR), Montréal, Canada*

(Accepted December 22, 2013. First published online: January 28, 2014)

SUMMARY
To assist physically disabled people with impaired upper limb function, we have developed a new 7-DOF exoskeleton-type robot named *Motion Assistive Robotic-Exoskeleton for Superior Extremity* (*ETS-MARSE*) to ease daily upper limb movements and to provide effective rehabilitation therapy to the superior extremity. The ETS-MARSE comprises a shoulder motion support part, an elbow and forearm motion support part, and a wrist motion support part. It is designed to be worn on the lateral side of the upper limb in order to provide naturalistic movements of the shoulder (vertical and horizontal flexion/extension and internal/external rotation), elbow (flexion/extension), forearm (pronation/supination), and wrist joint (radial/ulnar deviation and flexion/extension). This paper focuses on the modeling, design, development, and control of the ETS-MARSE. Experiments were carried out with healthy male human subjects in whom trajectory tracking in the form of passive rehabilitation exercises (i.e., pre-programmed trajectories recommended by a therapist/clinician) were carried out. Experimental results show that the ETS-MARSE can efficiently perform passive rehabilitation therapy.

KEYWORDS: Robotic exoskeleton; Nonlinear control; Physical disability; Passive rehabilitation; Upper limb impairment.

1. Introduction

Upper limb impairment (such as full or partial loss of function in shoulder joint, elbow joint, and wrist joint movements) is very common in the elderly, but can also be a secondary effect due to strokes, cardiovascular diseases, trauma, sports injuries, occupational injuries, and spinal cord injuries. A proper functioning of the upper limb is very important for the performance of essential daily activities. According to the World Health Organization, each year strokes and cardiovascular diseases affect more than 15 million people worldwide.[5] Of these, 85% of stroke survivors incur acute arm impairment, and 40% are chronically impaired or permanently disabled, thereby placing burden on the family and community.[8] Rehabilitation programs are the main method to promote functional recovery in these subjects.[11] Since the number of such cases is constantly growing, and the treatment duration is long, requiring skilled therapists or clinicians, introducing robots could therefore significantly contribute to the success of these programs in providing very efficient passive and tireless rehabilitation for long a period of time as the proposed *Motion Assistive Robotic-Exoskeleton for Superior Extremity* (*ETS-MARSE*) demonstrates.

It has been shown in several studies that intensive and repetitive therapies significantly improve motor skills.[13] Further studies have revealed that enhanced motor learning occurs when patients

* Corresponding author. E-mail: mhrahman@ieee.org

practice a variety of functional tasks[14–18] (such as reaching movements) and receive feedback intermittently (e.g., visual and haptic feedback in virtual reality).[9,15–18,20–22] Therefore, these key factors of therapy are to be integrated in rehabilitation paradigms, and this can be done through rehabilitation robotics. Moreover, recent studies also reveal that robot-aided therapy and virtual reality-based rehabilitation significantly reduce arm impairment[9,15–18,20–23] and improve motor function, allowing the subject to regain upper limb function of motion.[24,25]

To assist physically weakened and/or disabled individuals with impaired upper limb function, extensive research has been carried out in many branches of robotics, particularly on wearable robot (e.g., exoskeletons, powered orthotic devices, etc.) and/or end-effector-based robotic devices (i.e., devices which do not actively support or hold the subject's arm but connect with the subject's hand or forearm).[24,26–28] The exoskeleton-type robotic devices found in literature are either chair-[30,31] or floor-mounted,[19,29,32] but the end-effector devices are commonly found as floor-/desk-mounted. Table I highlights and compares some features (e.g., degrees of freedom (DOFs), sensors and actuators used, placement of actuators, actuation mechanism, therapeutic regime) of these devices.

Although much progress has been made in robotics, we are still far from the desired objective, as existing robots are not yet able to restore bodily mobility or function. This is due to limitations in the area of proper hardware design and that of control algorithms in terms of developing intelligent and autonomous robots that perform intelligent tasks. Some of the notable hardware limitations in the existing exoskeleton systems include limited degrees of freedom and range of motion[3,9,27,31] as compared with that of human upper extremities, robust and complex structures,[12] weak joint mechanisms of the exoskeleton system,[30,31] bulky actuated joints,[17] relatively heavy weight of the exoskeleton arm,[17,32] lack of proper safety measures and compensation for gravity forces,[12,26,27,31] and complex cable routing for transmission mechanisms.[6,9,30] The ETS-MARSE developed in this research has taken the above limitations into account, and is designed based on upper limb joints movement; it has a relatively low weight, can be easily fitted or removed, and is able to effectively compensate for gravity. Moreover, to avoid the complex cable routing encountered in many exoskeleton systems,[6,9,30] an innovative gear transmission mechanism has been developed for forearm pronation/supination and shoulder joint internal/external rotation. Note that cable transmission always adds some undesirable vibration and can loosen up during operation; therefore it should be avoided. Some devices used gear mechanism with a closed circular structure of forearm/upper arm cup.[19,30] However, it is unrealistic and inconvenient to insert and remove the arm through a closed circular structure.

Although extensive research has been carried out in developing smart rehabilitative and motion-assistive devices, a few numbers of such devices can be found in the literature that focused on the passive rehabilitation approach. The passive arm movement therapy is considered as a first stage of physiotherapy treatment (exercise) that is usually given to the patients to improve passive range of movements (ROMs). Therefore, this therapeutic approach should be given utmost importance.

Table II briefly summarizes and compares some features of existing robotic devices that focused on passive rehabilitation therapy. It can be seen from Table II that the weight of the ETS-MARSE arm from shoulder joint to wrist handle is 7.072 kg. Compared with the existing exoskeleton devices having at least shoulder and elbow motion support parts and focused on passive and/or active rehabilitation approach, the developed ETS-MARSE is found to be light in weight. For example, weight of CADEN-7 (7 DoFs, focused on passive rehabilitation, but not verified experimentally) is 9.2 kg excluding the weight of actuators. The exoskeleton was primarily developed for human power assist and uses cable mechanism to transmit power to the joints. The inherited problems in cable-driven systems is already discussed. Other passive rehabilitation robotic devices, such as iHandRehab,[4] IntelliArm,[7] and Hand Motion Assist Robot,[10] only focused on the hand and wrist rehabilitation. Soft-actuated exoskeleton,[12] though have 7 DoFs, it uses pneumatic muscle actuators, and therefore requires cumbersome experimental setup to operate. Moreover, the exoskeleton structure comprises week joint mechanism and suffers from safety issues. Also, it can be seen from Table II that the majority of exoskeleton systems uses proportional integral and derivative (PID)-based control approach, meaning that dynamic models of the system as well as that of human upper limb were ignored. Our developed ETS-MASRE designed to provide every variety of movements to the upper extremity also addressed the control issue and has used model-based control approach.

Most of the existing rehabilitative devices, although having limited degrees of freedom, demonstrated robot-assisted active rehabilitation exercises.[36,39] Note that passive arm movement therapy is the very first type of physiotherapy treatment given to the subjects/patients who are unable

https://doi.org/10.1017/S0263574714000034 Published online by Cambridge University Press

Table I. State of the art.

Exoskeleton robot for upper limb rehabilitation						
Project/institute /researcher/year	Active DOFs	Sensors	Actuators	Placement of actuators	Actuation mechanism	Therapeutic regime
			Floor-/Desk-mounted			
ExoRob, 2010[1,2]	4	Force, torque	Brushless DC motors	Joint	Gear drive	Elbow, wrist, forearm
ABLE, CEA-LIST, 2008[3]	4	Force	DC Faulhaber	Remote	Ball-screw and cable	Shoulder, elbow
CADEN-7, University of Washington, 2007[6]	7	Force, EMG	Rare earth brushed motors	Joint and remote	Gear drive, cable	Shoulder, elbow, forearm, wrist
L-EXOS, PERCRO, 2009[9]	5	Force	DC servo	Joint and remote	Gear drive, cable	Shoulder, elbow, forearm
Soft-actuated exoskeleton, University of Salford[12]	7	Strain gauge	Pneumatic muscle actuators	Remote	Linkage, cable	Shoulder, elbow, forearm, wrist
MGA exoskeleton (Carignan et al., 2009)[19]	6	Force	Brushless DC motors	Joint	Gear drive	Shoulder, elbow, wrist
Nagai et al., Ritsumeikan University 1998[29]	8	Force	DC servo	Joint and remote	Linkage, direct drive	Shoulder, elbow, forearm, wrist
ARMin-III, Swiss Federal Institute of Technology, 2009[33]	4	Force	Brushed motors	Joint and remote	Gear drive, belt drive, cable	Shoulder, elbow
MAHI exoskeleton, Rice University, 2006[17]	5	Force	Frameless electrical motors	Joint	Direct drive, parallel mechanism	Elbow, forearm, wrist
Noritsugu and Tanaka, Okayma University, 1997[32]	2	Force	Pneumatic rubber muscle	Remote	Linkage, cable	Shoulder, elbow
			Chair-mounted			
SUEFUL-7, Saga University, 2009[30]	7	Force, EMG	DC servo motors	Joint and remote	Gear drive, cable	Shoulder, elbow, forearm, wrist
MULOS, University of Newcastle, 1997[34]	5	Pressure, force	Electric motors, hydraulic actuator	Joint and remote	Gear drive, hydraulic transmission, linkage	Shoulder, elbow
Pneu-WREX, 2005[35]	5	-	Pneumatic	Remote	Linkage	Shoulder, elbow, wrist

Table I. Continued.

End-effector-based rehabilitative device						
Project/device /references	Brief description /therapeutic regime	Arm support	Sensors	Actuation mechanism	Actuator	Control
MIT-MANUS (InMotion)[28,36]	The 1st version of this device used a 2-DOF planar shoulder and elbow robot to provide therapy of stroke victims. A later version of which includes wrist module for whole arm rehabilitation[28,36].	Forearm, wrist	Force	Crank and slider mechanism	Brushless motor	IMC
REHAROB system[37]	The REHAROB therapeutic system used two industrial robots (each having 6 DOFs) to provide passive physiotherapy for shoulder and elbow joint movements for patients with spastic hemiparesis	Upper arm, forearm	Force, torque	Orthosis instrumented with robot	Electric motor	IFC
iPAM system[26]	This system uses a dual robotic arm (each having three active DOFs) to deliver therapy via two orthoses located on the upper arm and wrist of the subjects	Upper arm, wrist	Force	Pneumatic actuation	Pneumatic	ADC
HWARD[27]	This system is a 3-DOFs desk-mounted pneumatically actuated device that was developed to assist the subject's hand in grasp and in release movements	Wrist	Pressure	Linkage	Pneumatic	PneC
Hand exoskeleton[38]	The exoskeleton was designed for pinching movement (index finger and thumb) assistance. Skin surface EMG signals were used to control the exoskeleton	Wrist	EMG & touch sensors	Linkage & cable mechanism	Pneumatic	BCA, VCA
ARM guide[41]	The ARM guide was designed to assist in reaching movements, in both horizontal and vertical directions	Forearm	Force, torque	Linkage	DC servo motor	PD
MIME system[44]	The system incorporated a PUMA-260 robot and two commercial mobile arm supports modified to limit arm movement to the horizontal plane (2D); a later version uses PUMA-560 to provide therapy in 3D workspace	Forearm	Force	Linkage mechanism with PUMA	Servomotor	PFC

Table I. Continued.

End-effector-based rehabilitative device						
Project/device /references	Brief description /therapeutic regime	Arm support	Sensors	Actuation mechanism	Actuator	Control
ARCMIME[45]	The device was developed from the concept MIME system.[44] Clinical studies revealed that the ARCMIME is able to replicate the movements and data of subjects with neurological impairment	Forearm	Force, torque	Gear and link	Coreless DC servomotor	Same as MIME
Homma and Arai, AIST, 1995[31]	The system used a parallel mechanism to suspend upper arm at the elbow and wrist level.	Forearm, wrist	–	Cable mechanism	Electric motor	–
GENTLE/s system[22]	The system utilizes an active 3-DOF HapticMaster robot that connects the subject's arm through a wrist orthosis and uses virtual reality (VR) technologies to deliver therapy.	Through wrist orthosis	Force, tactile	Cable mechanism	DC motor	BP

ADC = admittance control; IFC = indirect force control; IMC = impedance control; PneC = pneumatic control; PD = proportional derivative; BCA = binary control algorithm; VCA = variable control algorithm; PFC = position feedback control; BP = bead pathway.

Table II. State of the art, passive rehabilitative devices.

Name/Year	DOFs	Therapeutic regime	Weight (kg)	Control	Placement	Actuation mechanism	Experimental validation of passive exercises
ETS-MARSE – present research	7	Shoulder, elbow, forearm, wrist	7.07*	CTC	Floor-mounted	Gear drive	Yes, all joints' movements
iHandRehab, 2011[4]	8	Fingers	0.250†	–	Desk-mounted	Gear drive, parallelogram mechanism	No
IntelliArm, 2009[7]	8	Shoulder, elbow, wrist, finger	–	–	Floor-mounted	Cable and link mechanism	Yes, but only fingers
Hand motion assist robot, 2007[10]	18	Wrist, hand	–	PD	Desk-mounted	Cable and link mechanism	Yes, only fingers
CADEN-7, 2007[6]	7	Shoulder, elbow, forearm, wrist	9.2‡	PID	Floor-mounted	Gear drive, cable	No
Soft-actuated exoskeleton, 2003[12]	7	Shoulder, elbow, forearm, wrist	2.0**	PID	Desk-mounted	Linkage, cable	Yes, but only elbow

Control: CTC = computed torque control, PID = proportional integral & derivative control.
*Shoulder joint to wrist (Fig. 2, point-M to knuckle), including actuators weight.
†Only the weight of the exoskeleton structure (i.e., weight of the actuators and their fixtures are not considered).
‡Shoulder joint to wrist excluding actuator weight.
**Only the exoskeleton structure. The system uses pneumatic muscle actuators, therefore it required cumbersome experimental setup to operate.

to actively move their arms throughout their complete range of motion following a surgery[40] of the shoulder-, elbow-, or wrist joint due to joint dislocation, or as a result of a stroke mostly due to spasticity and increased muscle tone.[42,43] Therefore, this issue should be properly addressed in rehabilitation robotics. As a solution to this issue, in this paper we have also presented a control strategy with nonlinear computed torque control technique to provide passive rehabilitation therapy for single- and multi-joint movements.

In our previous research, we developed exoskeleton-type robots for rehabilitation to assist elbow-, forearm-,[1] and wrist joint movements.[2] In a continuing effort toward providing movement assistance to the whole arm (shoulder, elbow, forearm, and wrist joint) in this research, we have focused on the development of an innovative new 7-DoF exoskeleton-type robot (ETS-MARSE).

The paper presents a complete bio-mechatronic system that includes (i) mechanical design of the ETS-MARSE; (ii) electrical and electronic design of the ETS-MARSE; (iii) control strategy to maneuver the ETS-MARSE; and (iv) experiment results demonstrating passive upper limb rehabilitation exercises with the developed ETS-MARSE.

The ETS-MARSE was designed based on upper limb articulations and movement. Modified Denavit–Hartenberg (DH) conventions[48] were used in developing the kinematic model. In dynamic modeling and control, subject parameters as well as the ETS-MARSE parameters, such as arm length, mass of different segments, robot arm link lengths, and inertia, were estimated according to the upper limb properties of a typical adult.[46] The ETS-MARSE is supposed to be worn on the lateral side of the upper arm, with the aim of providing effective rehabilitation for the shoulder joint (3 DOFs: horizontal and vertical motion, flexion/extension motion, and internal/external rotation), elbow joint (1 DOF: flexion/extension motion), forearm (1 DOF: pronation/supination motion), and wrist joint (2 DOFs: flexion/extension motion and radial/ulnar deviation) movements. The entire ETS-MARSE is manufactured using aluminum, which gives the structure a relatively lightweight. Brushless DC motors incorporated with harmonic drives (HD) are used to actuate the ETS-MARSE. Note that HDs are compact in shape, low in weight, have low/zero backlash properties, and also are back-drivable.[33,47] As the ETS-MARSE will be in direct contact with a human subject (i.e., robot user), mechanical stoppers are added to each rotational joint to limit its movement within the anatomical range of the human upper limb.[46]

The actuation mechanisms developed for the shoulder joint's internal/external rotation (1 DOF) support part and the forearm motion support part (1 DOF) are somewhat complex as it is practically impossible to place any actuator along the axis of rotation of the upper arm (e.g., with the humerus/radius) due to the anatomical configuration of the human arm. Moreover, as the ETS-MARSE will be worn on the lateral side of the arm, there will be an offset between the upper arm axis of rotation and the actuator axis of rotation. Although in gear mechanisms actuators can be placed at a certain offset (eccentricity) with respect to the desired axis of rotation (for instance, axis of rotation of forearm), such a mechanism is not suitable for our purposes because in this case meshing gears are supposed to rotate around a physical axis of rotation (e.g., shaft). We are unable to fit such a mechanical shaft along the line of axis of upper arm motion (e.g., with the humerus/radius). Therefore, we have introduced and developed an alternate gear mechanism where motion is transmitted from an anti-backlash gear (mounted on a motor shaft) to an open-type, custom-made meshing ring gear attached rigidly to the upper arm cup. This gear mechanism is discussed in Section 2.2.

In the next section a detailed overview of the development of the ETS-MARSE is presented. In Section 3, experimental results are presented to evaluate the performance of the ETS-MARSE with regard to passive rehabilitation, and finally in Section 4 the paper ends with the conclusion and the future works.

2. Exoskeleton Robot, ETS-MARSE

To rehabilitate and ease human upper limb movement, the proposed 7-DOF ETS-MARSE is modeled based on the concept of human upper limb articulations and movement. Considering the safety of robot users, and to provide assistance in performing essential daily activities, e.g., eating, reaching tasks, grasping, combing, washing the body, etc., preliminary studies on the anatomical range[46] of the upper limb movements have been carried out in order to choose a suitable movable range for the ETS-MARSE. This movable range is depicted in Fig. 1.

https://doi.org/10.1017/S0263574714000034 Published online by Cambridge University Press

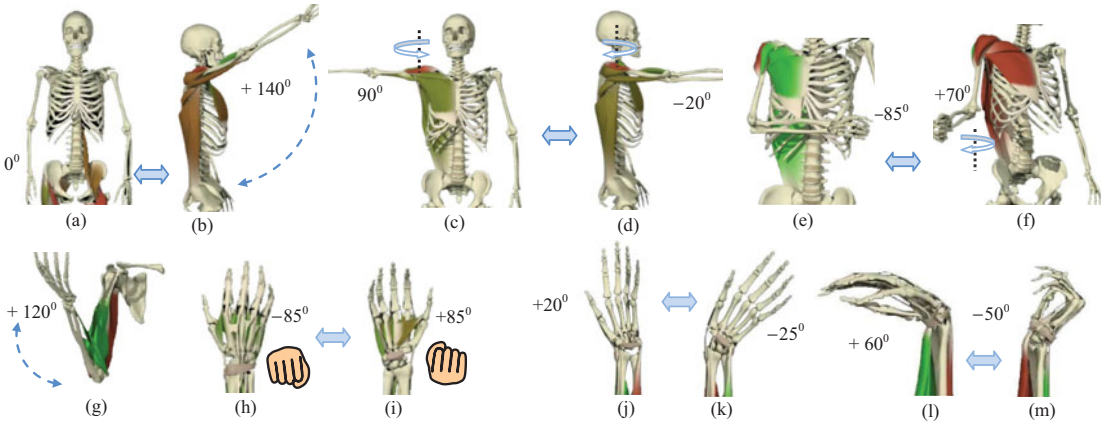

Fig. 1. (Colour online) Movable range of proposed ETS-MARSE. (a) Initial (zero) position; (b) shoulder joint: vertical flexion, (c) shoulder joint: horizontal extension; (d) shoulder joint: horizontal flexion; (e) shoulder joint: internal rotation; (f) shoulder joint: external rotation; (g) elbow flexion; (h) forearm pronation; (i) forearm supination; (j) radial deviation; (k) ulnar deviation; (l) wrist flexion; (m) wrist extension.

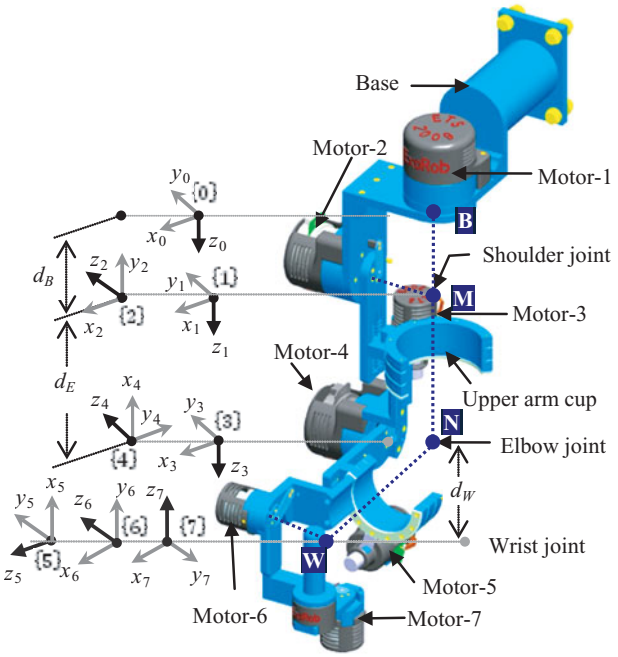

Fig. 2. (Colour online) Link frame attachments of the ETS-MARSE.

2.1. Kinematic model

To develop the kinematic model of the ETS-MARSE, the link-frame attachments are depicted in Fig. 2. The joint axes of rotation of the human upper limb corresponding to the proposed ETS-MARSE are indicated by dark black arrow heads (i.e., *Z*-axes). In this model, joints 1, 2, and 3 together constitute the glenohumeral joint (GHJ), commonly known as the shoulder joint (Fig. 2, point-M), where joint 1 corresponds to horizontal flexion/extension, joint 2 corresponds to vertical flexion/extension, and joint 3 to internal/external rotation. Note that for this exoskeleton robot, the axes of joints 1, 2, and 3 (i.e., Z_{1-3}) intersect at a common point. The axes of joints 4 and 5 are also intersecting at a common point (point-N, Fig. 2) at a distance d_E (length of humerus) from GHJ. It should also be noted that joint 4 corresponds to flexion/extension of the elbow joint, and joint 5 corresponds to pronation/supination of the forearm. As shown in Fig. 2, joints 6 and 7 intersect at

https://doi.org/10.1017/S0263574714000034 Published online by Cambridge University Press

Table III. Modified Denavit–Hartenberg parameters.

Joint (i)	α_{i-1}	a_{i-1}	d_i	θ_i
1	0	0	d_B	θ_1
2	$\pi/2$	0	0	θ_2
3	$\pi/2$	0	d_E	θ_3
4	$-\pi/2$	0	0	θ_4
5	$\pi/2$	0	d_W	θ_5
6	$-\pi/2$	0	0	$\theta_6 - \pi/2$
7	$-\pi/2$	0	0	θ_7

α_{i-1} is the link twist, a_{i-1} corresponds to link length, d_i stands for link offset, and θ_i is the joint angle of the ETS-MARSE.

Table IV. Mass and inertia* properties of the ETS-MARSE.

Segment (Fig. 2)	Segment length (cm)	Segment weight (kg)	Center of gravity, CG (cm)			Moment of Inertia, I (kg.m^2)		
			CG_X	CG_Y	CG_Z	Ixx	Iyy	Izz
Shoulder joint*	14.0	3.47	0.007	–13.82	–9.84	0.0232	0.0148	0.013
Upper arm†	25.0 ± 8.85	3.737	–1.31	–9.79	19.5	0.0233	0.0128	0.020
Forearm‡	26.0 ± 4.75	2.066	–2.93	–16.32	5.89	0.0166	0.0100	0.0126
Joints 6 & 7	Point-W (Fig. 2)	0.790	–0.035	–12.18	4.17	0.0029	0.0019	0.0012
Hand**	7.75 ± 4.75	0.495	6.22	0.00	5.00	0.0010	0.0012	0.0003

*Point-B to Point-M (Fig. 2); †Point-M to Point-N (Fig. 2); ‡Elbow to wrist (joint-6); **joint-7 to knuckle. The mass and inertia properties of the ETS-MARSE were estimated from the CAD modeling using Pro/Engineer software.

another common point (wrist joint; point-W, Fig. 2) at a distance d_W (length of radius) from the elbow joint. Joint 6 corresponds to radial-ulnar deviation, and joint 7 corresponds to flexion/extension.

To obtain the DH parameters, we assume that coordinate frames (i.e., the link-frames which map between the successive axes of rotation) coincide with the joint axes of rotation and have the same number of orders, i.e., frame $\{1\}$ coincides with joint 1, and frame $\{2\}$ with joint 2, and so on. The modified DH parameters corresponding to the placement of link frames (in Fig. 2) are summarized in Table III. These DH parameters are used to get the homogeneous transfer matrix,[48] which represents the positions and orientations of the reference frame with respect to the fixed reference frame $\{0\}$, which is located at distance d_B from the first reference frame $\{1\}$.

2.2. Mechanical design

The 7-DOF ETS-MARSE (as shown in Fig. 2) comprises the following three parts: shoulder motion support, elbow and forearm motion support, and wrist motion support. The entire ETS-MARSE arm is fabricated with aluminum to provide the exoskeleton structure with a relatively lightweight, since aluminum is a low density material having reasonable strength characteristics. The mass and inertia properties of the ETS-MARSE are presented in Table IV. Compared with the existing exoskeleton devices,[33,47] the developed ETS-MARSE is found to be light in weight.

Shoulder motion support: The shoulder joint motion support part has 3 DOFs. To assist with horizontal and vertical flexion/extension motion, it consists of two motors, two links (link-A, and link-B), and two potentiometers. Link-A holds motor-1 at one of its ends (Fig. 3(a)), and is rigidly attached to the base structure of the robot (Fig. 2) at its other end. As shown in Fig. 3(a), link-B, which is hinged with motor 1 and carries motor-2 on its other end, is "L"-shaped in order to accommodate the subject's shoulder joint. Therefore, the axes of rotation of motors 1 and 2 are supposed to intersect at the center of rotation of the subject's shoulder joint. Moreover, by adjusting the seating height (e.g., using a height-adjustable chair) it would be easy to align the center of rotation of the shoulder joint of the subject to that of the ETS-MARSE. Here it is worth mentioning that there is no scapular elevation, but rather rotation during the abduction of the GHJ.[49] However, the scapular elevation of subjects, which is common due to the GHJ flexion, will normally be allowed during the vertical flexion motion of the developed ETS-MARSE, and there will be no discomfort to the subject if the

https://doi.org/10.1017/S0263574714000034 Published online by Cambridge University Press

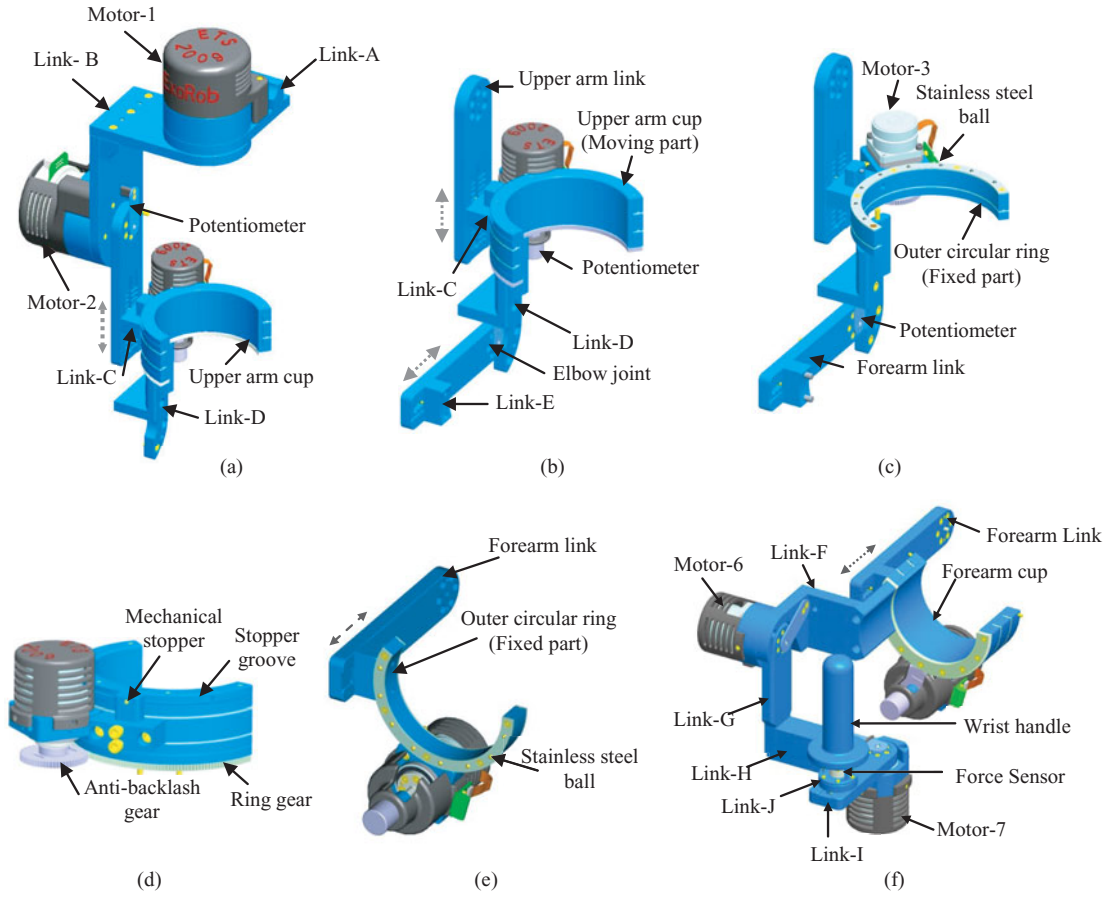

Fig. 3. (Colour online) (a) Shoulder motion support part; (b) Internal/external rotation support part (when elbow motor is unplugged from elbow joint); (c) showing custom-made, open-type bearing when upper arm cup is not assembled; (d) actuation mechanism for shoulder joint's internal/external rotation; (e) forearm motion support part (when the forearm cup is not assembled); (f) wrist motion support part (2 DOFs).

center of rotation of the shoulder joint of the subject is aligned with that of the ETS-MARSE. Note that motor-1 is responsible for shoulder joint horizontal flexion/extension motion and motor-2 for vertical flexion/extension motion.

To assist with the shoulder joint's internal/external rotation, the ETS-MARSE comprises an upper arm link, a sliding link (link-C), a fixed link (link-D), a motor, a custom-made open-type bearing, a ring gear, an anti-backlash gear, and a potentiometer. The upper arm link as shown in Fig. 3(b) is hinged with motor-2 (Fig. 3(a)) and holds the entire ETS-MARSE arm. Link-C (Figs. 3(a) and (b)) is rigidly attached to the outer circular ring, and is able to slide along the upper arm link (Fig. 3(b), dotted arrow) so that the distance between the upper arm cup and the shoulder joint (as well as the distance between the elbow joint and the shoulder joint) may be adjusted to accommodate a wide range of users. The outer circular ring, as depicted in Fig. 3(c), is designed to hold stainless steel balls (4-mm diameter) on its both sides. These balls are positioned between the grooves of the inner and outer circular rings, and act as a frictionless rotating mechanism. The open half-circular structure of the upper arm cup allows users to position the arm easily, without having to insert it through a closed circular structure. As depicted in Fig. 3(c), motor-3 is rigidly mounted on the back of the fixed outer ring. Figures 3(c) and (d) show the anti-backlash gear, which is clamped along the motor shaft to transmit the rotary motion to the ring gear. Note that the open ring gear is firmly attached to the upper arm cup and is responsible for rotating the upper arm cup over the custom-designed open-type bearing.

Elbow and forearm motion support: The elbow motion support part comprises a forearm arm link, a fixed link (link-D), a motor, and a potentiometer. As shown in Fig. 3(b), link-D acts as a bridge

https://doi.org/10.1017/S0263574714000034 Published online by Cambridge University Press

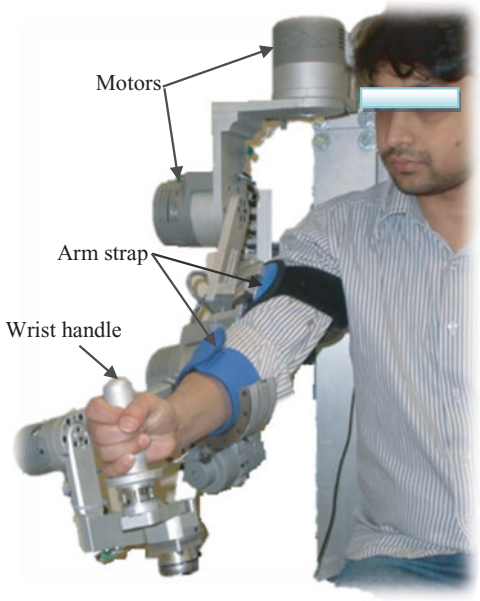

Fig. 4. (Colour online) ETS-MASRE with its user.

between the shoulder joint internal/external rotation support part and the elbow motion support part. Its one end is assembled with the upper arm cup, and with the other end it holds the elbow motor and the elbow motion support part of the ETS-MARSE. The forearm link, as depicted in Fig 3(e), is hinged with the elbow motor at the elbow joint (Fig. 2) and carries the entire forearm motion support part (Fig. 3(e)).

The forearm motion support part consists of a sliding link (link-E), a motor, a custom-made open-type bearing, a ring gear, an anti-backlash gear, and a potentiometer. The sliding link (link-E) is rigidly attached to the outer circular ring, and is able to slide along the forearm link (Fig. 3(e), dotted arrow) to adjust the distance between the forearm strap and the elbow joint (as well as to adjust the distance between the elbow joint and the wrist joint). Like the upper arm cup, the open half circular structure of the forearm cup allows users to place and position their forearm easily, without having to insert it through a closed circular structure. As shown in Fig. 2, motor-5 is rigidly mounted on the back of the fixed outer circular ring (Fig. 3(e)). The actuation mechanism of the forearm motion support part is quite similar to that of the shoulder joint internal/external support part, and as a result we have excluded a detailed description of the forearm motion support part. Note that to hold the upper arm/forearm in a proper position, soft arm straps (Fig. 4) are pasted on the upper arm and forearm cups.

Wrist motion support: The wrist motion support part (as shown in Fig. 3(f)), has 2 DOFs: one for assisting *radial/ulnar deviation*, and the other for assisting *flexion/extension* motion. To assist in the movement of radial/ulnar deviation (at the wrist joint), the proposed ETS-MARSE comprises a fixed link (link-F), a motor, and a potentiometer. Link-F (as shown in Fig. 3(f)) is rigidly attached to the forearm cup, and holds motor-6 at its other end, which corresponds to joint 6 (radial/ulnar deviation) of the ETS-MARSE.

The flexion/extension motion support part of the wrist joint consists of three fixed links (G, H, and I), one sliding link (link-K), a motor, a potentiometer, and a wrist handle. As shown in Fig. 3(f), link-G is hinged with joint-6, and holds the flexion/extension motion support part of the wrist joint. Link-H at its one end is attached to link-G and rigidly holds motor-7 on its other end. As shown in Fig. 3(f), link-I is hinged to motor-7 and carries the wrist handle on its other end. A sliding link (link-J) is positioned between link-I (Fig. 3(f)) and the wrist handle, which allows an adjustment of the distance between the wrist joint and the wrist grip.

To ensure the safety of the robot users, mechanical stoppers are added at each joint to limit the angle of rotation within the range of anatomical joints limits.[46] Note that these mechanical stoppers are adjustable, and therefore can be adjusted according to patients' active/passive ROMs. For instance,

https://doi.org/10.1017/S0263574714000034 Published online by Cambridge University Press

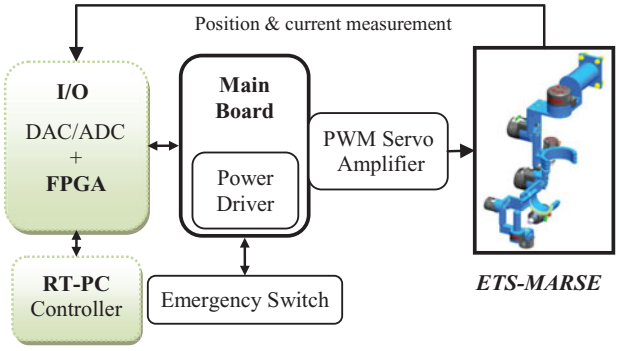

Fig. 5. (Colour online) Electrical-electronic configuration.

although the ROM of the ETS-MARSE at the level of shoulder joint internal/external rotation is 70° to –85°, it can be adjusted to any value within the range, e.g., 45° to –45°, or 40° to –70° etc. An emergency switch is also installed to cut off the power should the need arises. On top of these, *hardware safety features* and *software safety features* were added in the control algorithm, which include limiting the joints' range of movements depending on patient requirements, limiting the joints' speed, limiting the joints' torques, motor currents, and finally limiting the voltage values, which are the final output of the controller and the command values of motor drivers.

In the passive therapeutic approach (where the ETS-MARSE was maneuvered to follow pre-programmed trajectories representing passive rehabilitation exercises) the type of robot-aided rehabilitation exercises, the duration of therapy, and execution speed of such exercises are chosen by a therapist or clinician. Therefore, in this case, patient's safety (which includes ROM and speed of movement) while using the ETS-MARSE is ensured by a therapist/clinician in addition to the mechanical and software safety features (limiting the joints' range of movements) included in the ETS-MARSE.

On the other hand, in the active rehabilitation approach, where the ETS-MARSE is maneuvered by the user input wrist force sensor command to assist or guide the subject in performing some specific tasks, such as grasping or reaching, safety of the subject is also ensured with several software safety features as mentioned previously in addition to mechanical stoppers. For instance, we have limited the velocity of joints' movements up to ± 100°/s so that the undesired input force commands from the user cannot drive the ETS-MARSE very fast. Also, the torque saturation limits, as mentioned above, should prevent the joints' torques not to exceed beyond the safe driving limit, which may often be resulted due to sudden perturbation, jerking, or impact to the wrist force sensors. Moreover, voltage and current saturation limits were added in the control algorithm to ensure the safety of motor drivers as well as actuators.

Detailed specifications of the ETS-MARSE are given in Table V. It should be mentioned here that the low friction properties of the exoskeleton joints together with the drives' backdrivability[33,47] properties have made the system backdrivable. Therefore, one may be able to manipulate the ETS-MARSE by simply moving the wrist handle.

2.3. Electrical and electronic design

The electrical and electronic configuration for the ETS-MARSE system is depicted in Fig. 5. It consists of a CPU processor with a reconfigurable field-programmable gate array (FPGA), a main board, seven motor driver cards, and a real-time (RT) PC. The FPGA unit has two ethernet ports (10/100 Mb/s), which are used for communication with RT-PC via TCP/IP.

The main board as shown was designed to have slots for motor driver cards, only one of which is depicted in Fig. 5. Note that as a safety feature, an emergency stop switch was installed with the board to cut off power in case any emergency. The motor driver cards, which carry the motor drivers, were custom-designed to fit in the slots of the main board. The drivers used are type PWM servo amplifiers specially designed to drive brushless DC motors at high switching frequency (33 kHz) (specifications: reference voltage: ± 15 VDC; analog output: ± 10 VDC; maximum continuous current: ± 6 A). As the controller deals with the dynamics of the 7-DOF ETS-MARSE,

https://doi.org/10.1017/S0263574714000034 Published online by Cambridge University Press

Table V. ETS-MARSE at a glance.

Material: aluminum	DOFs: 7			Actuators: DC servomotor		
Range of movements (degrees)						
Joint-1	Joint-2	Joint-3	Joint-4	Joint-5	Joint-6	Joint-7
–20 to 90	0 to 140	–85 to 60	0 to 120	–85 to 85	–25 to 20	–50 to 60

Actuators, Maxon (brushless)		
Specification	EC-90, flat 90 W (joints 1, 2, 4)	EC-45, flat 30 W (joints 3, 5–7)
Nominal voltage (V)	24	12
Nominal speed (rpm)	2650	2860
Torque constant (mNm/A)	70.5	25.5
Weight (g)	648	88

Harmonic drives			
Specification: CSF-	2UH17–120 F (joints 1, 2)	2XH14–100 F (joint 4)	2XH11–100 F (joints 3, 5–7)
Torque at 2000 rpm (Nm)	24	7.8	5
Momentary peak torque (Nm)	86	54	25
Repeated peak torque (Nm)	54	28	11
Gear ratio	120	100	100

Anti-backlash gear and ring gear (pressure angle: 20^0, pitch: 32)			
	Anti-backlash gear	Ring gear	
Specification	(joints 3, 5)	Joint-3	Joint-5
Number of teeth	62	186	155
Bore diameter (inch)	0.2498	4.724	3.74

Force sensors, ATI, MINI40E*				
Axes:	Fx, Fy (±N)	Fz (±N)	Tx, Ty (±Nm)	Tz (±Nm)
	80	240	4	4

*A high linearity 6-axis force sensor (Mini40E, ATI) is instrumented underneath the wrist handle to measure the instantaneous reaction force. This signal will be used to actuate ETS-MARSE in order to provide active assistance (our next step of research).

to speed up the execution time (≤1 ms), an RT-PC was employed to deal with the control algorithm, leaving the tasks of data acquisition and internal current loop control to the FPGA.

2.4. Control

Given the dynamics of human arm movement, which is nonlinear in nature, in this paper we focused primarily on a nonlinear modified computed torque control technique to carry out some recommended passive rehabilitation exercises.

The dynamic behavior of the ETS-MARSE can be expressed by the well-known rigid body dynamic equation as

$$M(\theta)\ddot{\theta} + V(\theta, \dot{\theta}) + G(\theta) + F(\theta, \dot{\theta}) = \tau, \tag{1}$$

where $\theta \in \mathbb{R}^7$ is the joint angles vector, τ is the generalized torques vector, $M(\theta) \in \mathbb{R}^{7\times7}$ is the inertia matrix, $V\left(\theta, \dot{\theta}\right) \in \mathbb{R}^7$ is the Coriolis/centrifugal vector, $G(\theta) \in \mathbb{R}^7$ is the gravity vector, and

https://doi.org/10.1017/S0263574714000034 Published online by Cambridge University Press

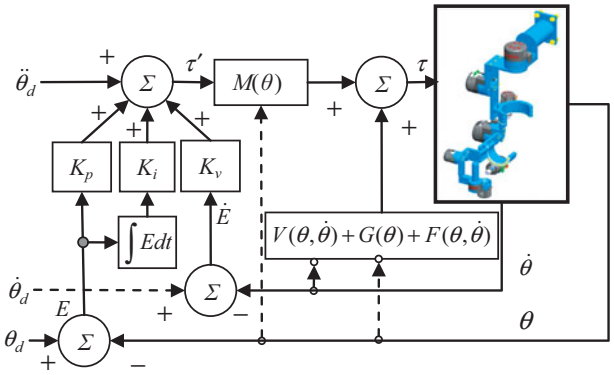

Fig. 6. (Colour online) Schematic diagram of modified computed torque control.

$F\left(\theta,\dot{\theta}\right) \in \mathbb{R}^7$ is the friction vector. Note that the friction vector is modeled as a nonlinear Coulomb friction, and can be expressed as

$$\tau_{\text{friction}} = F\left(\theta,\dot{\theta}\right) = csgn(\dot{\theta}), \tag{2}$$

where c is the Coulomb-friction constant. Equation (1) can be written as

$$\ddot{\theta} = -M^{-1}(\theta)\left[V(\theta,\dot{\theta}) + G(\theta) + F(\theta,\dot{\theta})\right] + M^{-1}(\theta)\,\tau. \tag{3}$$

$M^{-1}(\theta)$ always exists since $M(\theta)$ is symmetrical and positive definite. The layout of the modified computed torque control technique is depicted in Fig. 6. Unlike the conventional computed torque control approach, here we have added an integral term to have a better tracking performance and to compensate the trajectory tracking error that usually occurs due to imperfect dynamic modeling, parameter estimation, and also for external disturbances. The control torque in Fig. 6 can be written as

$$\tau = M(\theta)\left[\ddot{\theta}_d + K_v(\dot{\theta}_d - \dot{\theta}) + K_p(\theta_d - \theta) + K_i\int(\theta_d - \theta)\,dt\right] + V(\theta,\dot{\theta}) + G(\theta) + F(\theta,\dot{\theta}). \tag{4}$$

From relations (1) and (4), we may write:

$$\ddot{\theta} = \ddot{\theta}_d + K_v(\dot{\theta}_d - \dot{\theta}) + K_p(\theta_d - \theta) + K_i\int(\theta_d - \theta)\,dt, \tag{5}$$

where θ_d, $\dot{\theta}_d$, and $\ddot{\theta}_d$ are the desired position, velocity and acceleration, respectively, and K_p, K_v, and K_i are diagonal positive definite matrices. Let the error vector E and its derivative be:

$$E = \theta_d - \theta;\ \dot{E} = \dot{\theta}_d - \dot{\theta},\ \ddot{E} = \ddot{\theta}_d - \ddot{\theta}. \tag{6}$$

Therefore, relation (5) can be rewritten in the following form:

$$\ddot{E} + K_v\dot{E} + K_pE + K_i\int E\,dt = 0, \tag{7}$$

where the control gains K_p, K_v, and K_i are positive definite matrices. Therefore, a proper choice of these matrices ensures the stability of the system.

It should be mentioned here that the same control approach could be used to maneuver the robot to track both Cartesian and joint space trajectories. It can be seen from Fig. 6 that the controller inputs are the joint space variables $(\theta_d, \dot{\theta}_d, \ddot{\theta}_d)$, therefore an inverse kinematic solution is required to convert Cartesian variables to joint space variables, X_d, $\dot{X}_d$, $\ddot{X}_d$. The inverse kinematic solution of a

https://doi.org/10.1017/S0263574714000034 Published online by Cambridge University Press

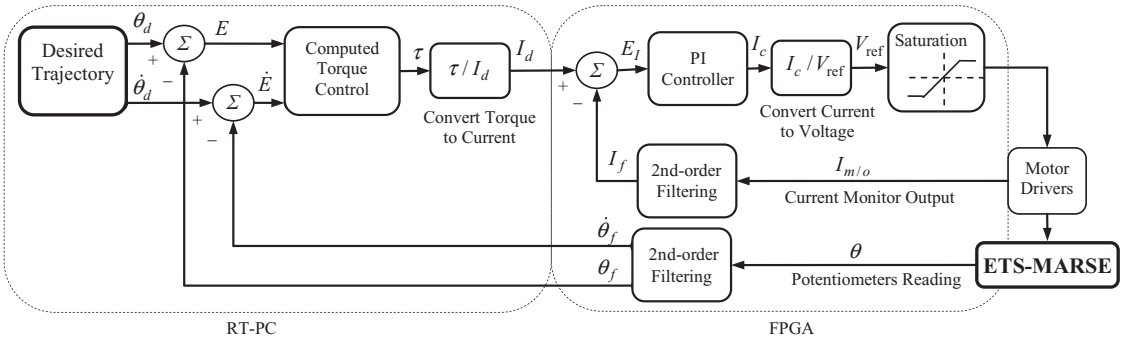

Fig. 7. Control architecture.

redundant manipulator (DOFs > 7) can be obtained by using the pseudo inverse of Jacobian matrix $J(\theta)$[50] as

$$\dot{\theta} = J^{\dagger}\dot{X}, \tag{8}$$

where $J^{\dagger} = J^{T}(JJ^{T})^{-1}$ is the pseudo inverse generalized.

The control architecture for the ETS-MARSE system is depicted in Fig. 7. The output of the controller is the joints torque commands. However, the torque commands are converted to motor currents, and finally to reference voltage as the voltage value is the drive command for motor drivers. Note that the computed torque controller updates the torque commands every 1 ms, and is executed in an RT-PC (Fig. 7, left dotted loop). Furthermore, to realize the RT control of the ETS-MARSE, and to ensure that the right control torque command is sent to the joints (as well as the reference voltage commands for the drivers), we also added a PI controller to minimize differences between desired and measured currents (i.e., the error command to PI controller). Note that the PI controller runs 10 times faster than the computed torque control loop, and is executed in the FPGA.

The current signals measured from the current monitor output of motor drivers are sampled at 0.1 ms, and are then filtered with a second-order filter with a damping factor $\zeta = 0.9$ and natural frequency $\omega_0 = 300$ rad/s prior to being sent to the PI controller. Filtering is important to eliminate high frequency or noisy data from the desired signals. Potentiometers at each joint are also sampled at 1 ms, and then filtered with the same second-order filter (with natural frequency, $\omega_0 = 30$ rad/s, damping factor, $\zeta = 0.9$) prior to being sent to the controller. Note that the friction vector of Eq. (4) is estimated by trial and error (i.e., by maneuvering the robot at different velocities).

3. Experiments and Results

In experiments, typical passive rehabilitation exercises for single (e.g., elbow joint movement) and multi-joint movements (e.g., reaching) were performed. Experiments were carried out with four healthy human subjects (mean ± SD, age: 27.8 ± 4.6 years; height: 176.75 ± 7.89 cm; weight: 81.25 ± 16.8 kg) where trajectories (i.e., pre-programmed trajectories recommended by a therapist/clinician[40]) tracking the form of passive rehabilitation exercises were carried out. Note that the desired trajectories and associated velocities were generated using the cubic polynomial approach.[48] The experiments were conducted on subjects in a seated position. Since the ETS-MARSE is mounted on a rigid base structure on the floor, wearing the ETS-MARSE arm will not impinge any load to the subjects. Further, the control algorithm is designed to compensate gravity loads efficiently and smoothly (mass of the ETS-MARSE arm and that of the upper limb).

Figure 8 demonstrates elbow joint flexion/extension motion, the very first type of passive rehabilitation exercises given to subjects to improve joint ROMs.[40,51] The topmost plot of Fig. 8 compares the desired joint angles (or reference trajectories, dotted line) with the measured joint angles (or measured trajectories, solid line). The intermediate row of the plot shows the tracking error as a function of time (i.e., deviation between desired and measured trajectories). It can be seen that the tracking error was quite small (<2°) and that the most noticeable was the steady state error (i.e., when the ETS-MARSE is maintaining the position of 90° against gravity), which lies below and/or

https://doi.org/10.1017/S0263574714000034 Published online by Cambridge University Press

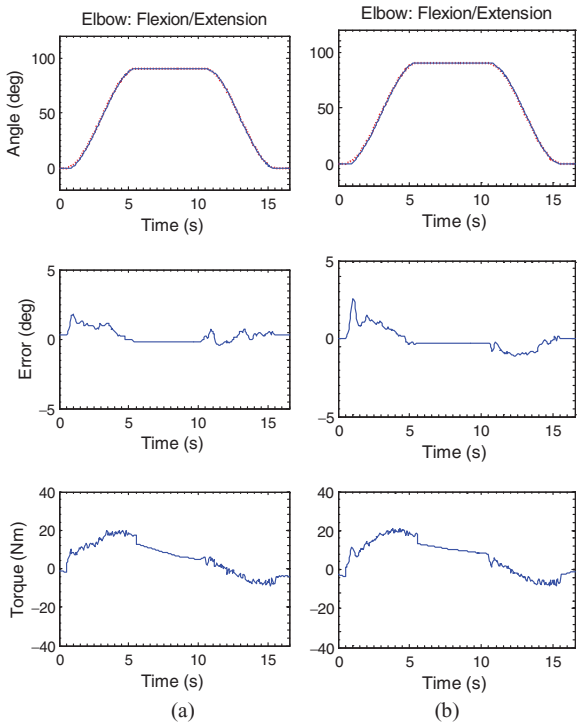

Fig. 8. (Colour online) Elbow joint flexion/extension. (a) Exercise was performed by subject-A having body weight of 63 kg and height of 165 cm. (b) Exercise was performed by subject-B having body weight of 100 kg and height of 180 cm.

close to 0.2° . The generated joint torques corresponding to the trajectory are plotted in the bottom row. Note that the control gains used for this control were found by trial and error, and are as follows:

$$K_P = diag[\,1000 \quad 700 \quad 115 \quad 800 \quad 1500 \quad 6000 \quad 750\,],$$
$$K_v = diag[\,100 \quad 120 \quad 15 \quad 110 \quad 100 \quad 300 \quad 110\,], \text{ and}$$
$$K_i = diag[\,100 \quad 800 \quad 300 \quad 800 \quad 1500 \quad 5000 \quad 1000\,].$$

To further evaluate the performance of the ETS-MARSE in gravity weight compensation while performing multi-joint movement exercise, another trial involving a cooperative movement of the elbow (flexion/extension) and shoulder joint internal/external rotation (Figs. 1(e) and (f)) was performed. As shown in Fig 10(a), the exercise begins with elbow flexion, and then repetitive internal/external rotation is performed (Fig. 9(b)); finally, the exercise ends with the extension of the elbow to 0° (Fig. 9(a)). Like previous trial, also in this case the tracking error (joint-4: $0.047^\circ \pm 0.19^\circ$; joint-3: $0.022^\circ \pm 0.56^\circ$) was found to be quite small. The steady state position error in this case was less than 0.1° .

Reaching movements are widely used and recommended[40] for multi-joint movement exercises. A straight-ahead reaching movement is depicted in Fig. 10, where the subject is supposed to slide his or her hand gently over the surface of a table, with the elbow initially at 90° . This movement is similar to dusting a table, which involves simultaneous and repetitive rotation at the elbow (extension) and shoulder joints. Typically this exercise is repeated 10 times,[40] and therefore a full cycle is depicted in Fig. 10. Note that to evaluate the robustness of the controller the same exercise was performed with three subjects. The mean and SD of the tracking errors for five different trials are summarized in Table VI.

Figure 11 demonstrates another typical rehabilitation exercise involving simultaneous motions of the elbow and the forearm. The objective of this task is to supinate the forearm from its initial position (Fig. 1(a)) to the fully supinated position while simultaneously flexing the elbow from complete extension to complete flexion, and next inversely moving the forearm from full supination

https://doi.org/10.1017/S0263574714000034 Published online by Cambridge University Press

Table VI. Mean tracking error (degree) and standard deviation, reaching movement exercise (Fig. 10).

	Subject-A				Subject-C				Subject-D			
	Joint-2		Joint-4		Joint-2		Joint-4		Joint-2		Joint-4	
Trials	Mean	SD	Mean	SD	Mean	SD	Mean	SD	Mean	SD	Mean	SD
1st	0.0255	0.311	0.0307	0.479	0.0223	0.3553	0.0343	0.498	0.0233	0.3858	0.0465	0.5155
2nd	0.033	0.329	0.0417	0.490	0.0187	0.395	0.0581	0.538	0.0059	0.4497	0.0800	0.6419
3rd	0.0329	0.334	0.0370	0.498	0.0299	0.409	0.0539	0.543	0.0207	0.470	0.0622	0.6728
4th	0.0285	0.357	0.0393	0.512	0.0229	0.406	0.0511	0.555	0.0269	0.4429	0.0528	0.6186
5th	0.0231	0.339	0.0323	0.506	0.0251	0.428	0.0489	0.580	0.0366	0.4147	0.0596	0.5834

Subject A: weight = 63 kg, height = 165 cm; Subject-C: weight = 72 kg, height = 180 cm; Subject -D: weight = 90 kg, height = 182 cm.

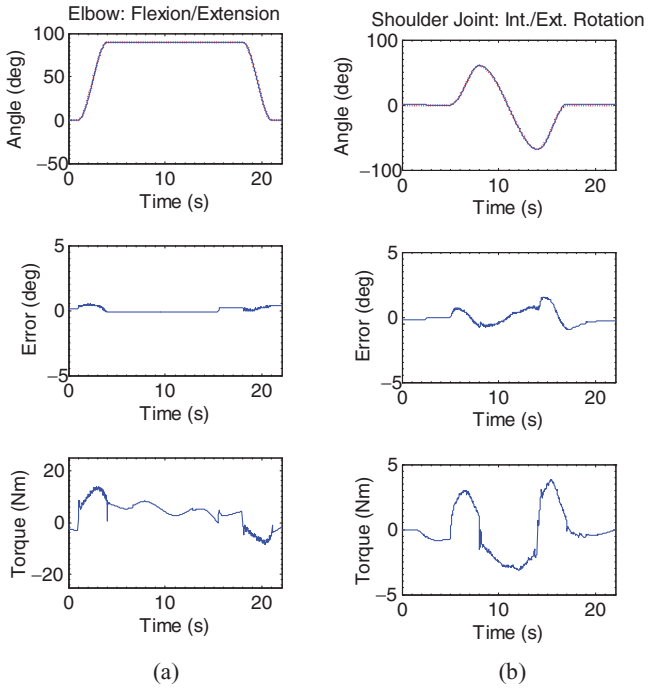

Fig. 9. (Colour online) Cooperative movement of elbow (joint-4) and shoulder joint (joint-3). (a) Elbow movement where the ETS-MARSE is supposed to flex from its initial position up to 90° position, and then maintain that position against the gravity. (b) Shoulder joint internal/external rotation.

to a full pronation position while the elbow simultaneously goes from complete flexion to extension. Controller tracking performance is certainly obvious from these figures as also in this case the tracking error was found to be small, which was less than 2.5°.

Finally, to evaluate the tracking performance of the whole system, an experiment involving simultaneous movements of all joints was performed. The schematic diagram of this exercise is depicted in Fig. 12. As seen in this figure, the exercise began at point-A with the elbow joint at 90° and then followed path AB to reach Target-1. The objective of this exercise is to reach different targets one after another, which involves movement of the entire upper limb's joints. It can be seen from this schematic that to reach different targets (located on the surface of the table, the exercise follows the path AB–BC–CD–DA. Experimental result of this trial is depicted in Fig. 13. It can be seen from the plots that the measured (solid line) and desired (dotted line) end point trajectories matched each other. The end-point tracking was found to be quite small in this case, which was below 1 cm.

We may conclude from all these results (Figs. 8 to 13) that ETS-MARSE can efficiently track desired trajectories, and thus should be adequate for the purpose of performing passive arm movement therapy.

https://doi.org/10.1017/S0263574714000034 Published online by Cambridge University Press

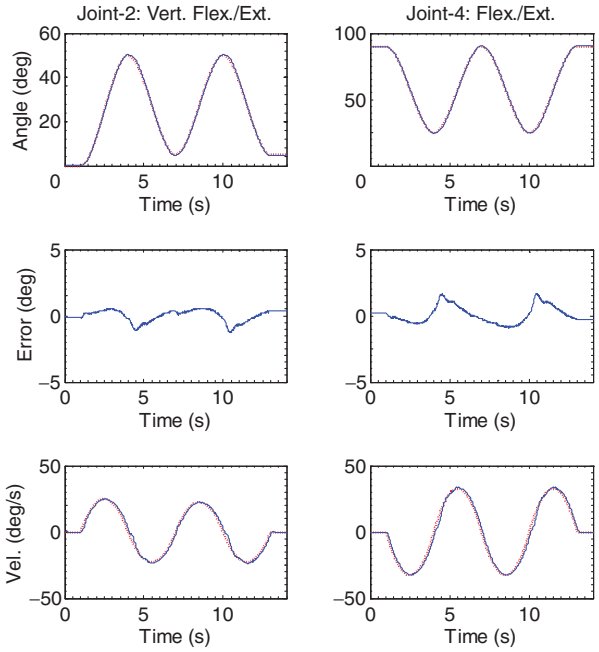

Fig. 10. (Colour online) Straight ahead reaching movement performed with subject-A. Combined movement of shoulder and elbow joint.

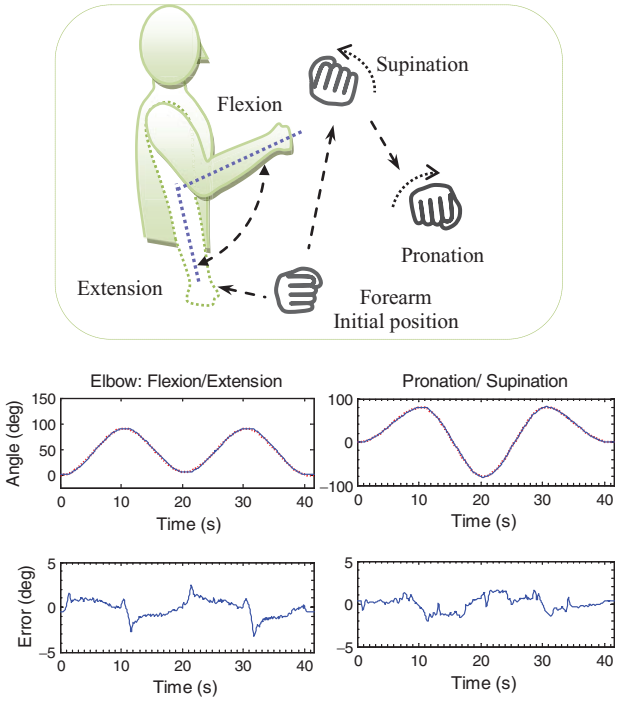

Fig. 11. (Colour online) Simultaneous movement of elbow and forearm.

4. Conclusions

A 7-DOF robotic exoskeleton, the ETS-MARSE, corresponding to the human upper limb has been developed to provide effective rehabilitation to people with disabilities at the levels of shoulder, elbow, forearm, and wrist joint movements. The trajectory tracking performance of the ETS-MARSE was evaluated through experiments. Such movements are widely used in physical therapy, and are performed very efficiently with the developed ETS-MARSE and the controller.

https://doi.org/10.1017/S0263574714000034 Published online by Cambridge University Press

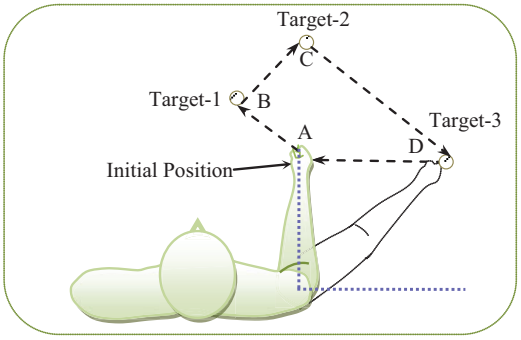

Fig. 12. (Colour online) Simultaneous movements of all joints (i.e., reaching movement exercise at different targets).

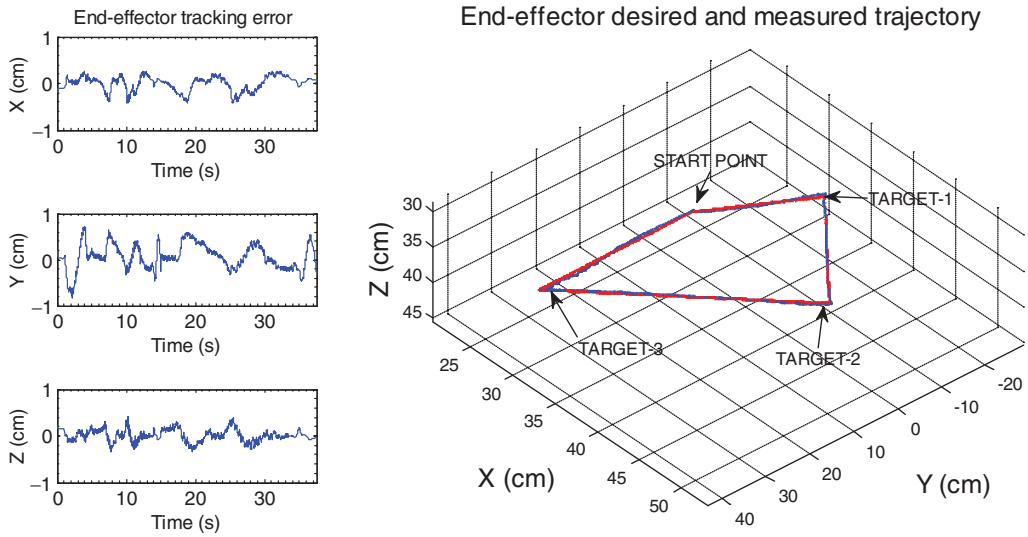

Fig. 13. (Colour online) Tracking performance evaluation for whole system. Endpoint movement at different targets (Cartesian trajectory tracking).

Future works will include the development of an electromyogram (EMG)-based controller to control the ETS-MARSE, as well as to provide an "active assisting mode of rehabilitation." Note that the EMG signal is generated biologically, and it reflects the user's true intention of motions.[30] Therefore, skin surface EMG signals should be used in RT control of the ETS-MARSE.

Acknowledgements

The first author gratefully acknowledges the support provided for this research through a FRQNT-B3 fellowship.

References

1. M. H. Rahman, M. Saad, J. P. Kenne and P. S. Archambault, "Robot-assisted rehabilitation for elbow and forearm movements," *Int. J. Biomechatronics Biomed. Robot.* **1**(4), 206–218 (2011).
2. M. H. Rahman, M. Saad, J. P. Kenne and P. S. Archambault, "Modeling and Development of an Exoskeleton Robot for Rehabilitation of Wrist Movements," *Proceedings of the 2010 IEEE/ASME International Conference on Advanced Intelligent Mechatronics (AIM 2010)*, Montreal, Canada (Jul. 6–9, 2010) pp. 25–30.
3. P. Garrec, J. P. Friconneau, Y. Measson and Y. Perrot, "ABLE, an innovative transparent exoskeleton for the upper-limb," *2008 IEEE/RSJ International Conference on Intelligent Robots and Systems*, Piscataway, NJ, (Sep. 22–26, 2008) pp. 1483–1488.

https://doi.org/10.1017/S0263574714000034 Published online by Cambridge University Press

4. J. Li, R. Zheng, Y. Zhang and J. Yao, "iHandRehab: An interactive hand exoskeleton for active and passive rehabilitation," *IEEE Int. Conf. Rehabil. Robot* , **2011**, 5975387 (2011) doi:10.1109/ICORR.2011.5975387.
5. J. Mackay and G. Mensah, *Atlas of Heart Disease and Stroke* (Nonserial Publication, World Health Organization, Brighton, UK, 2004).
6. J. C. Perry, J. Rosen and S. Burns, "Upper-limb powered exoskeleton design," *IEEE/ASME Trans. Mechatronics* **12**(4), 408–417 (2007).
7. R. Yupeng, P. Hyung-Soon and Z. Li-Qun, "Developing a Whole-Arm Exoskeleton Robot with Hand Opening And Closing Mechanism for Upper Limb Stroke Rehabilitation," *2009 IEEE International Conference on Rehabilitation Robotics: Reaching Users & the Community (ICORR '09)*, Piscataway, NJ (Jun. 23–26, 2009) pp. 761–765.
8. V. M. Parker, D. T. Wade and H. R. Langton, "Loss of arm function after stroke: Measurement, frequency, and recovery," *Int. Rehabil. Med.* **8**(2), 69–73 (1986).
9. A. Frisoli, F. Salsedo, M. Bergamasco, B. Rossi and M. C. Carboncini, "A force-feedback exoskeleton for upper-limb rehabilitation in virtual reality," *Appl. Bionics Biomech.* **6**(2), 115–126 (2009).
10. H. Kawasaki, S. Ito, Y. Ishigure, Y. Nishimoto, T. Aoki, T. Mouri, H. Sakaeda and M. Abe, "Development of a Hand Motion Assist Robot for Rehabilitation Therapy by Patient Self-Motion Control," *2007 IEEE 10th International Conference on Rehabilitation Robotics (ICORR '07)*, Piscataway, NJ (Jun. 12–15, 2007) pp. 257–263.
11. G. E. Gresham, D. Alexander, D. S. Bishop, C. Giuliani, G. Goldberg, A. Holland, M. Kelly-Hayes, R. T. Linn, E. J. Roth, W. B. Stason and C. A. Trombly, "American Heart Association Prevention Conference. IV. Prevention and rehabilitation of stroke. Rehabilitation," *Stroke* **28**(7), 1522–1526 (1997).
12. N. G. Tsagarakis and D. G. Caldwell, "Development and control of a 'soft-actuated' exoskeleton for use in physiotherapy and training," *Auton. Robot.* **15**(1), 21–33 (2003).
13. H. C. Huang, K. C. Chung, D. C. Lai and S. F. Sung, "The impact of timing and dose of rehabilitation delivery on functional recovery of stroke patients," *J. Chin. Med. Assoc.* **72**(5), 257–264 (2009).
14. C. J. Winstein, A. S. Merians and K. J. Sullivan, "Motor learning after unilateral brain damage," *Neuropsychologia* **37**(8), 975–987 (1999).
15. G. N. Lewis and J. A. Rosie, "Virtual reality games for movement rehabilitation in neurological conditions: How do we meet the needs and expectations of the users?" *Disabil. Rehabil.* **34**(22), 1880–1886 (2012).
16. D. A. Mauro, "Virtual Reality-Based Rehabilitation and Game Technology," *1st International Workshop on Engineering Interactive Computing Systems for Medicine and Health Care* (*EICS4Med*) Pisa, Italy (June 13, 2011) pp. 48–52.
17. C. Carignan, J. Tang and S. Roderick, "Development of an Exoskeleton Haptic Interface for Virtual Task Training," *2009 IEEE/RSJ International Conference on Intelligent Robots and Systems (IROS 2009)*, St. Louis, MO (Oct. 11–15, 2009) pp. 3697–3702.
18. M. Cameirao, S. Badia, E. Oller and P. Verschure, "Neurorehabilitation using the virtual reality based rehabilitation gaming system: Methodology, design, psychometrics, usability and validation," *J. NeuroEng. Rehabil.* **7**(1), 48 (2010).
19. A. Gupta and M. K. O'Malley, "Design of a haptic arm exoskeleton for training and rehabilitation," *IEEE/ASME Trans. Mechatronics* **11**(3), 280–289 (2006).
20. C. J. Winstein, J. P. Miller, S. Blanton, E. Taub, G. Uswatte, D. Morris, D. Nichols and S. Wolf, "Methods for a multisite randomized trial to investigate the effect of constraint-induced movement therapy in improving upper extremity function among adults recovering from a cerebrovascular stroke," *Neurorehabil. Neural. Repair* **17**(3), 137–152 (2003).
21. P. S. Lum, C. G. Burgar and P. C. Shor, "Evidence for improved muscle activation patterns after retraining of reaching movements with the MIME robotic system in subjects with post-stroke hemiparesis," *IEEE Trans. Neural Syst. Rehabil. Eng.* **12**(2), 186–194 (2004).
22. R. Loureiro, F. Amirabdollahian, M. Topping, B. Driessen and W. Harwin, "Upper limb robot mediated stroke therapy – GENTLE/s approach," *Auton. Robot.* **15**(1), 35–51 (2003).
23. G. B. Prange, M. J. Jannink, C. G. Groothuis-Oudshoorn, H. J. Hermens and M. J. Ijzerman, "Systematic review of the effect of robot-aided therapy on recovery of the hemiparetic arm after stroke," *J. Rehabil. Res. Dev.* **43**(2), 171–184 (2006).
24. H. I. Krebs, B. T. Volpe, M. L. Aisen and N. Hogan, "Increasing productivity and quality of care: Robot-aided neuro-rehabilitation," *J. Rehabil. Res. Dev*. **37**(6), 639–652 (2000).
25. S. W. Brose, D. J. Weber, B. A. Salatin, G. G. Grindle, H. Wang, J. J. Vazquez and R. A. Cooper, "The role of assistive robotics in the lives of persons with disability," *Am. J. Phys. Med. Rehabil.* **89**(6), 509–521 (2010).
26. P. R. Culmer, A. E. Jackson, S. Makower, R. Richardson, J. A. Cozens, M. C. Levesley and B. B. Bhakta, "A control strategy for upper limb robotic rehabilitation with a dual robot system," *IEEE/ASME Trans. Mechatronics* **15**(4), 575–585 (2010).
27. C. D. Takahashi, L. Der-Yeghiaian, V. Le, R. R. Motiwala and S. C. Cramer, "Robot-based hand motor therapy after stroke," *Brain* **131**(Pt 2), 425–437 (2008).
28. L. Masia, H. I. Krebs, P. Cappa and N. Hogan, "Design and characterization of hand module for whole-arm rehabilitation following stroke," *IEEE/ASME Trans. Mechatronics* **12**(4), 399–407 (2007).
29. K. Nagai, I. Nakanishi, H. Hanafusa, S. Kawamura, M. Makikawa and N. Tejima, "Development of an 8-DOF Robotic Orthosis for Assisting Human Upper Limb Motion," *1998 IEEE International Conference on Robotics and Automation*, Leuven, Belgium (1998) pp. 3486–3491.

30. R. A. R. C. Gopura, K. Kiguchi and L. Yang, "SUEFUL-7: A 7-DOF Upper-Limb Exoskeleton Robot with Muscle-Model-Oriented EMG-Based Control," *2009 IEEE/RSJ International Conference on Intelligent Robots and Systems (IROS 2009)*, Piscataway, NJ (Oct. 11–15, 2009) pp. 1126–1131.
31. K. Homma and T. Arai, "Design of an Upper Limb Motion Assist System with Parallel Mechanism," *Proceedings of the 1995 IEEE International Conference on Robotics and Automation. Part 1 (of 3)*, Nagoya, Japan (May 21–27, 1995) pp. 1302–1307.
32. T. Noritsugu and T. Tanaka, "Application of rubber artificial muscle manipulator as a rehabilitation robot," *IEEE/ASME Trans. Mechatronics* **2**(4), 259–267 (1997).
33. T. Nef, M. Guidali and R. Riener, "ARMin III – Arm therapy exoskeleton with an ergonomic shoulder actuation," *Applied Bionics Biomechanics* **6**(2), 127–142 (2009).
34. G. R. Johnson and M. A. Buckley, "Development of a New Motorised Upper Limb Orthotic System (MULOS)," *Proceedings of RESNA '97. Lets Tango – Partnering People and Technologies*, Arlington, VA (Jun. 20–24, 1997) pp. 399–401.
35. R. J. Sanchez, E. Wolbrecht, R. Smith, J. Liu, S. Rao, S. Cramer, T. Rahman, J. E. Bobrow and D. J. Reinkensmeyer, "A Pneumatic Robot for Re-Training Arm Movement After Stroke: Rationale and Mechanical Design," *International Conference on Rehabilitation Robot* (2005) pp. 500–504.
36. H. I. Krebs, B. T. Volpe, D. Williams, J. Celestino, S. K. Charles, D. Lynch and N. Hogan, "Robot-aided neurorehabilitation: A robot for wrist rehabilitation," *IEEE Trans. Neural Syst. Rehabil. Eng.* **15**(3), 327–335 (2007).
37. A. Tóth, G. Arz, G. Fazekas, D. Bratanov and N. Zlatov, "Post-Stroke Shoulder-Elbow Physiotherapy with Industrial Robots," **In**: *Advances in Rehabilitation Robotics, Human-Friendly Technologies on Movement Assistance and Restoration for People with Disabilities* (Z. Bien *et al.*, eds.) (Springer, Berlin, Germany, 2004) pp. 391–411.
38. L. Lucas, M. DiCicco and Y. Matsuoka, "An EMG-controlled hand exoskeleton for natural pinching," *J. Robot. Mechatronics* **16**(5), 482–488 (2004).
39. K. Kiguchi, M. H. Rahman and M. Sasaki, "Neuro-Fuzzy Based Motion Control of a Robotic Exoskeleton: Considering End-Effector Force Vectors," *Proceedings of the IEEE 2006 Conference on International Robotics and Automation*, Orlando, FL (May 15–19, 2006) pp. 3146–3148.
40. Brigham & Women's Hospital, "Physical therapy standards," Available at: http://www.brighamandwomens.org/Patients_Visitors/pcs/rehabilitationservices/StandardsofCare.aspx. Accessed January 19, 2014 (Jul. 7, 2011), online.
41. D. J. Reinkensmeyer, J. P. A. Dewald and W. Z. Rymer, "Guidance-based quantification of arm impairment following brain injury: A pilot study," *IEEE Trans. Rehabil. Eng* **7**(1), 1–11 (1999).
42. National Institute of Neurological Disorders and Stroke, *Post-Stroke Rehabilitation Fact Sheet* (NINDS, National Institutes of Health Bethesda, MD, 2011).
43. University of Virginia Health System, Spine Centre, *Nonoperative Treatment: Physical Therapy* (VCU Health System, Richmond, VA, 2011).
44. C. G. Burgar, P. S. Lum, P. C. Shor and H. F. M. Van der Loos, "Development of robots for rehabilitation therapy: The Palo Alto VA/Stanford experience," *J. Rehabil. Res. Dev.* **37**(6), 663–673 (2000).
45. R. M. Mahoney, H. F. M. V. D. Loos, P. S. Lum and C. Burgar, "Robotic stroke therapy assistant," *Robotica* **21**(1), 33–44 (2003).
46. N. Hamilton, W. Weimar and K. Luttgens, *Kinesiology: Scientific Basis of Human Motion*, XI ed. (McGraw-Hill, Boston, MA, 2008), xv + 627 pp.
47. C. Carignan, M. Liszka and S. Roderick, "Design of an Arm Exoskeleton with Scapula Motion for Shoulder Rehabilitation," *Proceedings of the 12th International Conference on Advanced Robotics (ICAR '05)* (Jul. 18–20, 2005) pp. 524–531.
48. J. J. Craig, *Introduction to Robotics: Mechanics and Control* (Pearson/Prentice Hall, Upper Saddle River, NJ, 2005) viii + 400 pp.
49. H. Hallaceli, M. Manisali and I. Gunal, "Does scapular elevation accompany glenohumeral abduction in healthy subjects?" *Arch. Orthop. Trauma Surg.* **124**(6), 378–381 (2004).
50. B. Siciliano, L. Sciavicco and L. Villani, *Robotics: Modelling, Planning and Control* (Springer, London, 2009) 666 pp.
51. K. Murray, "Stroke Rehab Exercises," available at: http://www.stroke-rehab.com/stroke-rehab-exercises.html. Accessed January 19, 2014 (2010), online.

https://doi.org/10.1017/S0263574714000034 Published online by Cambridge University Press